



HAL
open science

Reducing vertical acceleration in ballast layers of railways to mitigate geometrical disorders in high speed lines

Antoine Martin, Olivier Chupin, Jean Michel Piau, Pierre-Yves Hicher

► **To cite this version:**

Antoine Martin, Olivier Chupin, Jean Michel Piau, Pierre-Yves Hicher. Reducing vertical acceleration in ballast layers of railways to mitigate geometrical disorders in high speed lines. International Journal for Numerical and Analytical Methods in Geomechanics, 2017, 41 (12), pp.1349-1361. 10.1002/nag.2675 . hal-01630438

HAL Id: hal-01630438

<https://hal.science/hal-01630438>

Submitted on 2 Dec 2017

HAL is a multi-disciplinary open access archive for the deposit and dissemination of scientific research documents, whether they are published or not. The documents may come from teaching and research institutions in France or abroad, or from public or private research centers.

L'archive ouverte pluridisciplinaire **HAL**, est destinée au dépôt et à la diffusion de documents scientifiques de niveau recherche, publiés ou non, émanant des établissements d'enseignement et de recherche français ou étrangers, des laboratoires publics ou privés.

Reducing vertical acceleration in ballast layers of railways to mitigate geometrical disorders in high-speed lines

A. Martin^{1,2}, O. Chupin¹, J.-M. Piau¹ and P.-Y. Hicher³

¹*IFSTTAR, MAST, LAMES, F-44344 Bouguenais, France*

²*Eurovia Research Center, F-33703 Mérignac, France*

³*Research Institute in Civil and Mechanical Engineering, UMR CNRS 6183, Ecole Centrale de Nantes, F-44321 Nantes, France*

According to field feedbacks from high-speed lines (HSL), the increase of train operating speeds is responsible for unusual fast evolving geometrical disorders in ballasted tracks. This paper deals with the search of solutions applicable at the design stage to mitigate these disorders. The starting point of the present work relies on the assumption, comforted by the literature, of a strong correlation between disorders and vertical accelerations in the ballast layer induced by the train passages. This led us focus herein on the calculation and the analysis of accelerations in the railway structure. The vertical accelerations (γ_z) are computed using the in-house developed numerical program ViscoRail and on the basis of a reference HSL. These are shown to increase strongly with the train speed attesting to the link between the train speed and the geometrical disorders in ballast. Then, other simulations are run varying some structural parameters to evaluate their impact on the acceleration field γ_z . In that way, we show that decreasing the stiffness of the mechanical connection between the rails and the ballast, increasing the moment of inertia of the rails or the Young modulus of the sub-ballast layer, leads to a decrease of γ_z and could provide solutions for the design of future HSL. The solution consisting in the incorporation of an asphalt sub-ballast layer, as already experimented on sites, is finally examined in more details.

1. INTRODUCTION

The current context of environmental sustainability and of increasing traffic volume encourages the development and the modernization of public transportation. As regards to the high-speed rail field, this results in an increase of train speeds (over 300 km/h in France). However, this speed increase seems to be responsible for unusual fast evolving geometrical disorders (irreversible deformations) observed in the ballasted railway tracks. As a consequence, maintenance operations are more frequently required, in particular in the ballast layer, leading to higher direct and indirect costs.

To tackle this problem, a first approach, largely followed in the past, is based on the optimization of maintenance strategies with the practical aim of better planning maintenance operations. In terms of research, this has resulted in studying in the laboratory settlement laws for ballast under repeated loading to better predict the irreversible deformations of railway tracks. Since the first works by [1, 2] using a triaxial apparatus, more accurate laws have been established on the basis of tests performed at a reduced scale on track portions composed of one [3–5] or several sleepers [6, 7]. The results of the experiments conducted by Bodin and Al Shaer highlighted an amplification of the dynamic response of the track with the increase of the load frequency. The authors associated this phenomenon to rearrangements in the granular assembly. These results were confirmed by the works

by [8, 9] that showed a change of the ballast behavior as a function of the loading frequency, the highest frequencies possibly leading to a flow-like motion of the ballast material. Consequently, subsequent studies have incorporated in the aforementioned laws the important effect of speed or frequency on the settlement evolution. These laws were used in the context of high-speed lines (HSL) in [10, 11].

On the other hand, the present work is based on a different approach of the initial problem. Here, we rather focus on the possibility of innovative designs of HSL that may help mitigate by construction the geometrical disorders despite ever higher speeds. To accomplish this, we assume that the ballast grain motions are first of all related to the acceleration level undergone by the railway track under passing trains. The intuition is that short events of high vertical downward accelerations of the ballast layer can lead to temporary losses of confinement of the ballast granular assembly by decreasing its apparent weight (Section 2) and that it favors the grain displacements under mechanical loading leading to rapid settlements under the numerous repetitions of high-speed train passages.

This assumption provides the guideline of this paper, which is focused on the computation of the acceleration endured by the railway track and on ways to mitigate it. Thus, in Section 3, we briefly present the numerical tool that we developed specifically to compute the reversible dynamic response of a railway structure. In Section 4, we detail the typical response of a HSL computed for a reference case and the train speed $V=75$ m/s. In addition, this case can be considered as non-problematic in terms of maintenance according to field feedbacks. Hence, further in this paper, the computed accelerations for this case are set as thresholds to not be exceeded to warrant a safe behavior of infrastructures. Section 5 deals with a sensitivity analysis of the HSL response to several design parameters that can be used to make accelerations computed at $V > 75$ m/s go down the thresholds already defined. An example of innovative design of HSL incorporating a bituminous sub-layer is then studied in Section 6.

2. FOREWORDS ON THE EFFECT OF ACCELERATION ON THE STABILITY OF AN UNBOUND GRANULAR MATERIAL

The connection between the stability of a granular medium and the acceleration field to which it is submitted to may be illustrated through the bearing capacity of a semi-infinite medium composed of a Coulomb's friction material without cohesion. For a foundation of area S , the limit load F is given by the following relationship arising from dimensional analysis:

$$F_0 = S^{\frac{3}{2}} \rho g f(\phi) \quad (1)$$

in which ρ is the material density, ϕ its friction angle and g the standard gravity. This equation shows that F_0 is balanced by the inter-granular forces generated by the material own weight. Considering an additional homogeneous vertical acceleration field γ (positive downward) responsible for the field of inertia forces $-\rho\gamma$, the equation above, due to the non-discernibility of the effects between gravitational and inertial forces, becomes

$$F_\gamma = S^{\frac{3}{2}} \rho (g - \gamma) f(\phi) = F_0 \left(1 - \frac{\gamma}{g} \right) \quad (2)$$

This equation shows the 'destabilizing' effect of downward accelerations (in the extreme case of free fall, $F_\gamma=0$). Physically, this effect results in a loss of confinement of the granular medium and in a decrease of the contact inter-granular forces (normal forces, tangential friction forces). We believe that this phenomenon plays an important role in the aggravation of geometrical disorders observed on HSL as train speeds are increased. Consequently, we expect that reducing acceleration goes along with the mitigation of geometrical disorders. One aim of this paper is thus to quantify the acceleration field occurring in the railway structures when subjected to moving loads and try to reduce its intensity by acting on the design parameters.

3. VISCORAIL: A NUMERICAL PROGRAM FOR THE COMPUTATION OF THE DYNAMIC RESPONSE OF RAILWAYS

The simulations performed in this paper are focused on the computation of the dynamic response of railway structures to trains moving at constant speed. To accomplish this, we use a numerical program based on semi-analytical methods previously described in [12, 13].

For recall, the basic principle of this program, so-called ViscoRail, relies on a decoupling technique that consists in solving iteratively on one hand the track system composed of the rails and the sleepers and on the other hand the sub-structure modeled as a stack of semi-infinite layers (Figure 1). The connection between these two sub-systems is made through the pressure distribution, $p(x, t)$, at the surface of the sub-structure (i.e., at the interface between the sub-systems) which derives from the load transfer across the rail/sleeper system. The response of the whole system (track system plus sub-structure) is obtained after convergence of the iterative process that bears on $p(x, t)$. The rails are represented by Euler–Bernoulli beams tied to the sub-structure through springs of stiffness k_{spr} . The springs are located at the sleeper centers and account for the whole connection elements (pads and sleepers) between the rails and the sub-structure. In the model, the force in every spring is converted into a uniform pressure (vertical) that is applied on an area representing a sleeper imprint ($2a \times 2b$). The dynamic response of the sub-structure to an applied moving load is computed using the numerical program ViscoRoute© 2.0 [14–16], which is originally dedicated to pavements. Prior to using ViscoRoute© 2.0, an *ad hoc* decomposition of $p(x, t)$ on an infinite set of ‘loading waves’, each moving at a constant speed, is performed.

One feature of ViscoRail is the Huet–Sayegh constitutive law [17, 18] that can be used to model viscoelastic layers of the sub-structure. This law (Figure 2 and Eq. (3)) is particularly adapted to the modeling of asphalt materials and is further used in this paper to study the benefit, in terms of acceleration in the ballast, of incorporating a bituminous layer in the sub-structure.

$$E^*(\omega, \theta) = E_0 + \frac{E_\infty - E_0}{1 + \delta(j\omega\tau(\theta))^{-k} + (j\omega\tau(\theta))^{-h}} \quad (3)$$

E^* is the complex modulus of the material at frequency $f = \omega/2\pi$ and temperature θ . E_0 is the static elastic modulus, E_∞ is the instantaneous elastic modulus, k and h are exponents of the parabolic dashpots ($1 > h > k > 0$), and δ is a positive non-dimensional coefficient balancing the contribution of the first dashpot in the global behavior. Function $\tau(\theta)$ accounts for the equivalence principle between frequency and temperature. It is taken as

$$\tau(\theta) = \tau_0 \exp(A_1\theta + A_2\theta^2) \quad (4)$$

These parameters are usually determined from campaigns of complex modulus tests carried out at different frequencies and temperatures.

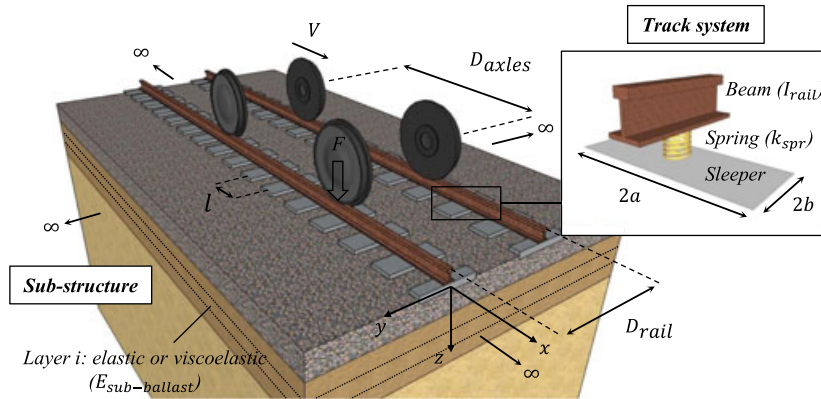


Figure 1. Railway track system under consideration ($z > 0$ downwards). [Colour figure can be viewed at wileyonlinelibrary.com]

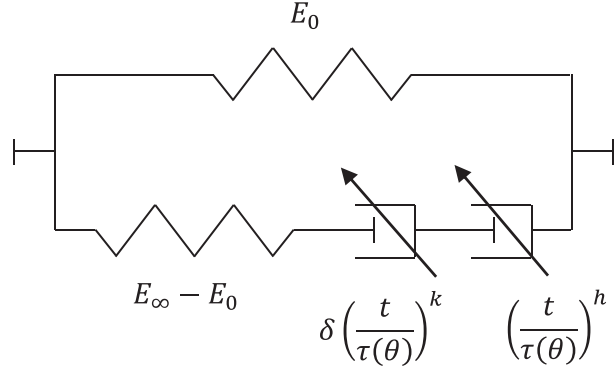


Figure 2. Schematic representation of the Huet–Sayegh rheological model (2 springs + 2 parabolic dampers with $0 < k < h < 1$).

4. DYNAMIC RESPONSE OF A CLASSIC ALL-GRANULAR HSL – STUDY OF A REFERENCE CASE

ViscoRail is first applied to compute the dynamic response of a reference case, which is assumed to be barely affected by the rapid deterioration of the ballast layer according to field feedbacks. This case refers to the structure described in Section 4.1 and is run for the reference speed of 270 km/h (75 m/s) reputed as less critical than the current operating speed of the order above 300 km/h (83 m/s). The dynamic response corresponding to this situation will serve further as a reference to define a threshold of acceptable vertical accelerations (γ_z) with regard to the ballast behavior.

We also take advantage of this structure to confirm the influence of speed on the dynamic response of the track bed.

4.1. Description of the reference case selected

The track bed of our reference case was defined from typical all-granular HSL structures encountered in France. It is composed of three elastic layers of which the properties are displayed in Table I. Note that the realistic set chosen for the Young moduli avoids (horizontal) tensile stress in the granular material layers.

The Young modulus and the moment of inertia (I_{rail}) of the rails modeled as Euler–Bernoulli beams are equal to 2.1×10^{11} Pa and 3×10^{-5} m⁴, respectively. The rails are spaced apart by $D_{\text{rail}} = 1.5$ m. The contact between the rails and the track bed is ensured by vertical springs of stiffness (k_{spt}) equal to 5×10^7 N/m. The dimensions of the sleeper prints at the surface of the track bed are $2a = 0.8$ m, $2b = 0.3$ m, and the center to center distance between two consecutive sleepers is $l = 0.6$ m (Figure 1). A bogie with four wheels moving at constant speed is applied on the rails, each wheel being represented by a vertical point force of constant amplitude $F = 8 \times 10^4$ N. The distance between both bogie axles (D_{axles}) is 3 m.

4.2. Reference computation ($V = 75$ m/s)

Figure 3a shows the typical 3D mapping of the vertical acceleration in the ballast layer for the wheels of the bogie located midway between two sleepers. As illustrated in this figure, upward accelerations

Table I. Properties of the track bed.

| | ρ (kg/m ³) | E ($\times 10^6$ Pa) | ν | Thickness (m) |
|-------------------|-----------------------------|-------------------------|-------|---------------|
| Ballast | 1800 | 150 | 0.4 | 0.3 |
| Sub-ballast layer | 1800 | 120 | 0.4 | 0.7 |
| Soil | 1800 | 100 | 0.4 | ∞ |

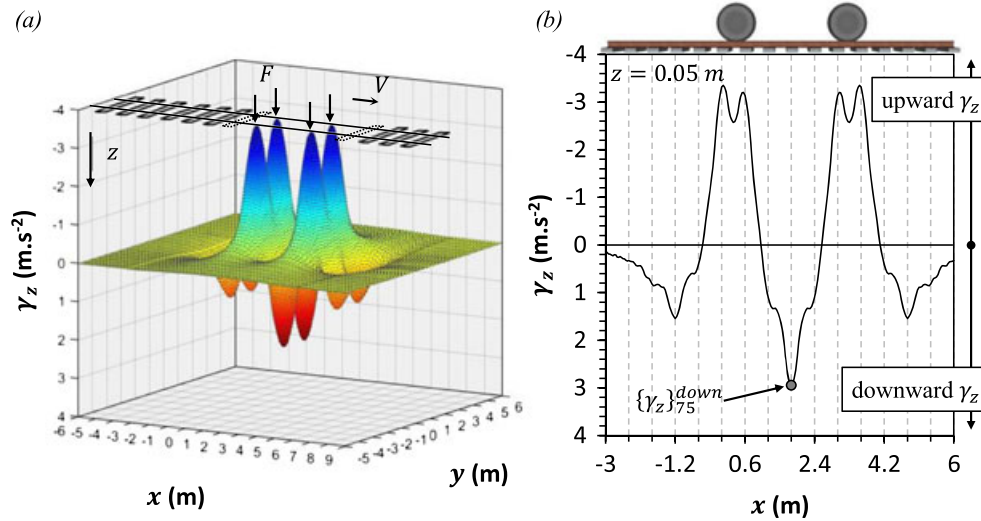


Figure 3. (a) Three-dimensional mapping of γ_z for a given position of the bogie ($V=75$ m/s). (b) Profile of vertical acceleration in the x direction near the track bed surface and under rail axis for the bogie axles located between sleepers. [Colour figure can be viewed at wileyonlinelibrary.com]

($\gamma_z < 0$) are located in the vicinity of the bogie axles, whereas downward γ_z are obtained between the bogie axles, as well as behind and ahead the bogie. Moreover, the higher amplitudes of γ_z in both directions are found under the rail axes. Hence, it was decided in the rest of the paper to plot γ_z as horizontal profiles in the x direction under a rail axis ($y=0$) and at a depth $z=0.05$ m, close to the free surface of the ballast layer.

In particular, Figure 3b gives the magnitude of the downward acceleration ($\{\gamma_z\}_{75}^{down} = 2.95$ m/s²) considered as acceptable in the following with regard to the ballast behavior.

4.3. Effect of speed on γ_z

The influence of speed on the acceleration field is confirmed by Figure 4 that shows two profiles of γ_z obtained for $V=75$ and 95 m/s.

As expected, the ratio between the maxima of γ_z at $V=95$ m/s and $V=75$ m/s (in both downward and upward directions) is close to the square speed ratio (Table II).

Actually, ratio 1.60 is that obtained from ViscoRail computations when taking negligible values of ρ for all the layers, indicating that the small difference with $\{\gamma_z\}_{95}/\{\gamma_z\}_{75} = 1.75$ is due to inertia effects in

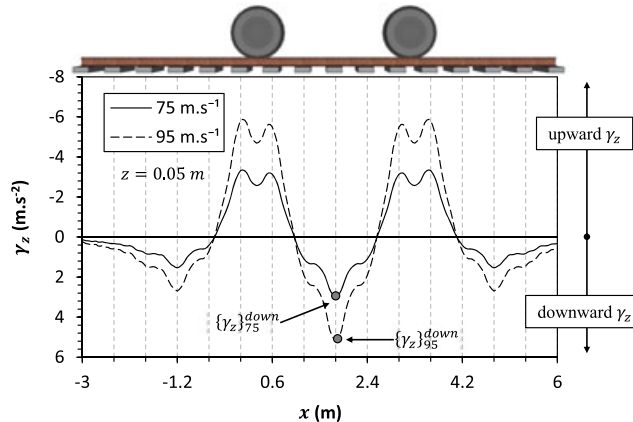


Figure 4. Comparison of γ_z between $V=95$ m/s and $V=75$ m/s. [Colour figure can be viewed at wileyonlinelibrary.com]

Table II. Ratio between the maximum of γ_z computed for $V=95$ and 75 m/s in both upward and downward directions and comparison with the square speed ratio.

| Direction | $\{\gamma_z\}_{75}$ (m/s ²) | $\{\gamma_z\}_{95}$ (m/s ²) | $\{\gamma_z\}_{95}/\{\gamma_z\}_{75}$ | $(95/75)^2$ |
|-----------|---|---|---------------------------------------|-------------|
| Upwards | -4.08 | -7.14 | 1.75 | 1.60 |
| Downwards | 2.95 | 5.15 | 1.75 | |

the structure. As shown by Figure 5, the difference between the computations performed with and without inertia forces logically grows with speed.

This shows that to a certain extent the computation of γ_z can be obtained from static calculations ignoring inertia forces in the track bed, especially in the context of comparative studies. This result (not used in this paper) can be useful to study complex situations (track bed geometry, nonlinear constitutive behavior, ...), which does not strictly respect the ViscoRail assumptions, by using finite element models for instance. Obviously, this simplified way of computing γ_z does not question the role and importance of γ_z itself on the stability of ballast as expressed by Eq. (2).

5. SENSITIVITY ANALYSIS OF γ_z WITH RESPECT TO RAILWAY DESIGN PARAMETERS

The aim of this section is twofold. One is to carry out a sensitivity analysis on γ_z with respect to railway design parameters. The other is to show how these results applied to our reference track bed can be used to reduce γ_z obtained at $V=95$ m/s to the level of that at 75 m/s.

Therefore, the sensitivity analysis is performed for $V=95$ m/s. Many factors were studied by means of numerical simulation [19] at this step, but only the most relevant are presented herein. These are the moment of inertia of the rails (I_{rail}), the stiffness of the vertical springs (k_{spr}) that ensure the connection between the rails and the track bed and the Young modulus of the sub-ballast layer ($E_{\text{sub-ballast}}$) (Figure 1). In the computations, these parameters are varied one at a time, the unchanged parameters being kept to the value of the reference case. The results of the sensitivity analysis are presented under the form of time evolutions of γ_z computed at a point located right under a sleeper center ($y=0, z=0.05$ m), which experiences the maximum acceleration in both downward and upward directions. Time $t=0$ corresponds to the rear axle of the bogie driven right above the observation point. In the next figures, the curve corresponding to the reference railway subjected to loads moving at 95 m/s is systematically plotted using a black continuous line, and the maximum of γ_z in the upward and downward directions obtained for $V=75$ m/s (Table II) are indicated by a horizontal straight line ($\{\gamma_z\}_{75}^{\text{up}}$ and $\{\gamma_z\}_{75}^{\text{down}}$ in the graphs).

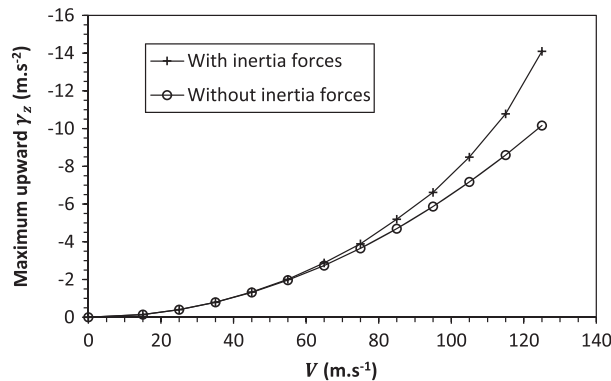


Figure 5. Maximum values of upward γ_z computed under a sleeper of the reference structure as a function of speed ($y=0, z=0.05$ m). Comparison of the results obtained with and without inertia forces.

5.1. Influence of k_{spr}

Figure 6 displays the results obtained for the following tested values of the spring stiffness: $k_{spr}=5 \times 10^7$ (reference), 4×10^7 , 3×10^7 , 2×10^7 , and 1×10^7 N/m. It appears that the maximum amplitude of γ_z decreases as the spring stiffness also decreases. This can be explained by the fact that for lower values of k_{spr} the distribution of the wheel loads is spread over a larger number of sleepers, leading to a decrease of the deflection and subsequently of the acceleration. For $k_{spr}=2 \times 10^7$ N/m, the maximum of γ_z is of the order of magnitude of that of the reference case $\{\gamma_z\}_{75}$.

Consequently, softening the connection between the rail and the track bed is a potential factor that could be used to mitigate the vertical accelerations in the ballast layer. In a practical way, this could be achieved by adding a flexible mat under the sleepers or by softening the pad between the rails and the sleepers.

5.2. Influence of I_{rail}

The tested values of I_{rail} are 3×10^{-5} (reference), 4×10^{-5} , 5×10^{-5} , 6×10^{-5} , and 7×10^{-5} m⁴. The results are presented in Figure 7. The same trend is observed when I_{rail} is increased as when k_{spr} is decreased because decreasing I_{rail} also leads to a distribution of the wheel loads over a larger number of sleepers.

This could be achieved by changing some geometrical characteristics of the rails. However, to reduce γ_z to the level of the reference case, I_{rail} must be multiplied by two. This might be difficult to reach in practice, but I_{rail} could be associated with other factors to make γ_z equal to or lesser than the threshold defined.

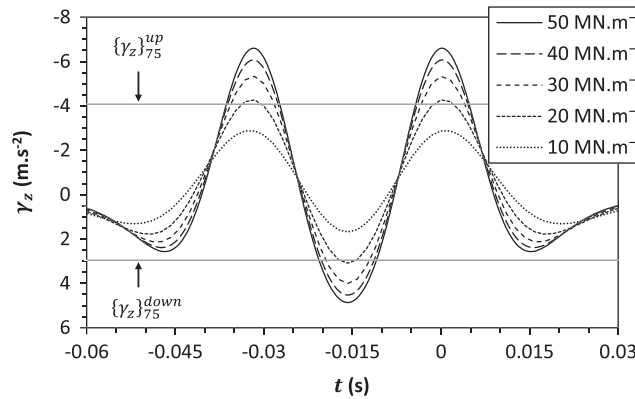


Figure 6. Time evolution of γ_z at a point located right under a sleeper center: influence of k_{spr} ($V=95$ m/s, $z=0.05$ m).

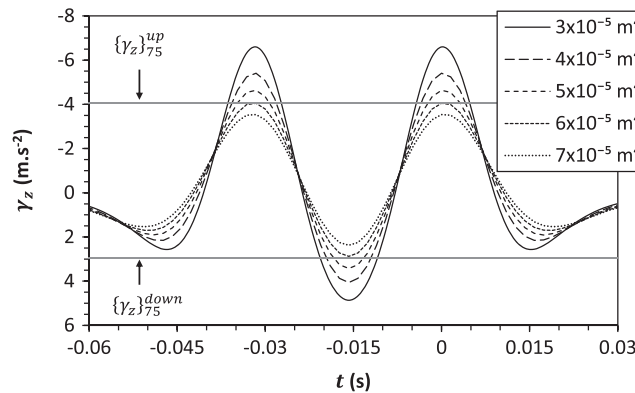


Figure 7. Time evolution of γ_z at a point located right under a sleeper center: influence of I_{rail} ($V=95$ m/s, $z=0.05$ m).

5.3. Influence of $E_{\text{sub-ballast}}$

The tested values of $E_{\text{sub-ballast}}$ are in the range of 120–650 MPa. For all these values, the aforementioned no-tensile stress criterion is respected in the granular layers and especially in the ballast layer. The results are displayed in Figure 8. It can be observed that an increase of $E_{\text{sub-ballast}}$ leads to a decrease of γ_z (in both the downward and upward directions). For $E_{\text{sub-ballast}}$ approximately equal to 500 MPa, the computed vertical acceleration is similar to that of the reference case.

Therefore, acting on $E_{\text{sub-ballast}}$ is another way to mitigate γ_z in the ballast layer that can result in particular from the use of bounded materials. Nonetheless, it is worth noting that the resulting stress developing in such materials would have to be investigated to evaluate their long-term behavior and performance with regard to fatigue damage.

5.4. Summary of the sensitivity analysis

Figure 9 summarizes the results of the sensitivity analysis with regard to the maximum downward acceleration, which is expressed as the ratio $R = \{\gamma_z\}_{95}^{\text{down}} / \{\gamma_z\}_{75}^{\text{down}}$. Abscissa δ in Figure 9 is the relative difference with respect to the reference case for a given design parameter ($\delta = \Delta k_{\text{spr}} / k_{\text{spr, ref}}$ or $\Delta I_{\text{rail}} / I_{\text{rail, ref}}$ or $\Delta E_{\text{sub-ballast}} / E_{\text{sub-ballast, ref}}$).

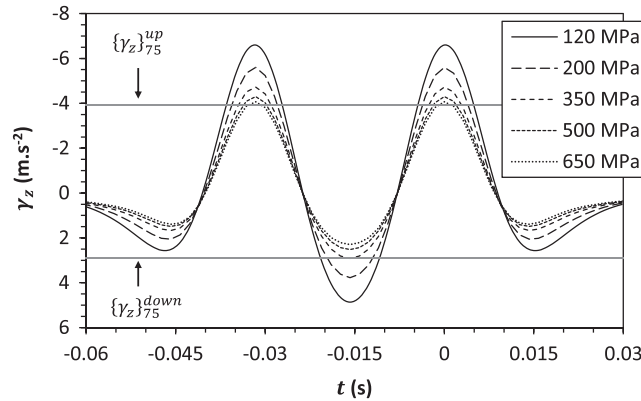


Figure 8. Time evolution of γ_z at a point located right under a sleeper center: influence of $E_{\text{sub-ballast}}$ ($V=95$ m/s, $z=0.05$ m).

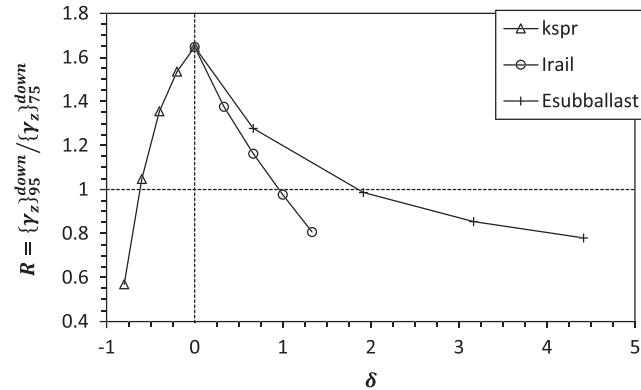


Figure 9. Ratio between the maximum γ_z computed for the different parameter values considered at $V=95$ m/s and that of the reference case ($V=75$ m/s).

Using the approximate differential of γ_z

$$\Delta\gamma_z \approx \frac{\partial\gamma_z}{\partial k_{\text{spr}}} \Delta k_{\text{spr}} + \frac{\partial\gamma_z}{\partial I_{\text{rail}}} \Delta I_{\text{rail}} + \frac{\partial\gamma_z}{\partial E_{\text{sub-ballast}}} \Delta E_{\text{sub-ballast}} \quad (5)$$

the previous sensitivity analysis can also be summarized by the following quantitative relationship:

$$\frac{\{\gamma_z\}_{95}^{\text{down}} - \{\gamma_z\}_{95,\text{new-struct}}^{\text{down}}}{\{\gamma_z\}_{75}^{\text{down}}} \approx -0.59 \frac{\Delta k_{\text{spr}}}{k_{\text{spr,ref}}} + 0.87 \frac{\Delta I_{\text{rail}}}{I_{\text{rail,ref}}} + 0.59 \frac{\Delta E_{\text{sub-ballast}}}{E_{\text{sub-ballast,ref}}} \quad (6)$$

which *a priori* indicates that combinations of the previous design parameters can be considered to mitigate γ_z . $\{\gamma_z\}_{95,\text{new-struct}}^{\text{down}}$ denotes the expected acceleration computed at speed $V=95$ m/s after changing the design parameters of the reference structure according to Δk_{spr} , ΔI_{rail} , and $\Delta E_{\text{sub-ballast}}$ where $\Delta(\text{param}) = (\text{param new struct}) - (\text{param ref struct})$.

5.5. Application to HSL design with operating speed of 95 m/s

As an example, the accuracy of Eq. (6) is evaluated by comparison to direct ViscoRail calculations performed for different sets of the design parameter values selected so as to decrease $\{\gamma_z\}_{95}^{\text{down}}$. Five computations are run assuming homothetic relative variations of the parameters ($-\Delta k_{\text{spr}}/k_{\text{spr,ref}} = \Delta I_{\text{rail}}/I_{\text{rail,ref}} = \Delta E_{\text{sub-ballast}}/E_{\text{sub-ballast,ref}} = |\delta| = 0.1$ to 0.5). A sixth calculation is performed for $-\Delta k_{\text{spr}}/k_{\text{spr,ref}} = 0.2$, $\Delta I_{\text{rail}}/I_{\text{rail,ref}} = 0$ and $\Delta E_{\text{sub-ballast}}/E_{\text{sub-ballast,ref}} = 0.4$.

Table III shows that in all cases the approximate value $\{\gamma^{\text{app}}\}_{95}^{\text{down}}$ differs no more than 10% from the direct computation of $\{\gamma_z\}_{95}^{\text{down}}$.

Then Eq. (6) can be used as a guide to adapt the reference structure of Section 4 to an operating speed of 95 m/s without exceeding the acceleration threshold obtained at $V=75$ m/s (as a reminder, ratio $\{\gamma_z\}_{95}/\{\gamma_z\}_{75}$ was found equal to 1.75 in both downward and upward directions in Section 4.3). By setting $\{\gamma_z\}_{95,\text{new-struct}}^{\text{down}} \leq \{\gamma_z\}_{75}^{\text{down}}$, the change in the design parameters should verify the condition:

$$-0.79 \frac{\Delta k_{\text{spr}}}{k_{\text{spr,ref}}} + 1.16 \frac{\Delta I_{\text{rail}}}{I_{\text{rail,ref}}} + 0.79 \frac{\Delta E_{\text{sub-ballast}}}{E_{\text{sub-ballast,ref}}} \geq 1 \quad (7)$$

For a homothetic variation, this condition is met for $|\delta| = 36\%$.

6. HSL INCORPORATING A BITUMINOUS MATERIAL UNDER THE BALLAST LAYER

Railway track beds incorporating a layer of asphalt paving material has become a common consideration for the construction of new HSL [20, 21]. Nonetheless, to our knowledge, few studies only have focused on the effect of using bituminous layers on the dynamic response of a railway, and the modeling of such structures is barely considered in the specialized literature. Then, taking advantage of the capabilities of ViscoRail to account for viscoelastic layers in a structure, the

Table III. Comparison between $\{\gamma^{\text{app}}\}_{95}^{\text{down}}$ and $\{\gamma_z\}_{95}^{\text{down}}$ (m/s^2) for the various sets of the design parameter values considered.

| | Homothetic | | | | | | Non-homothetic |
|---|------------|------|------|------|------|------|----------------|
| | 0 (ref.) | 10 | 20 | 30 | 40 | 50 | # |
| $k_{\text{spr}} (\times 10^7 \text{ N/m})$ | 5 | 4.5 | 4 | 3.5 | 3 | 2.5 | 4 |
| $I_{\text{rail}} (\times 10^{-5} \text{ m}^4)$ | 3 | 3.3 | 3.6 | 3.9 | 4.2 | 4.5 | 3 |
| $E_{\text{sub-ballast}} (\text{MPa})$ | 120 | 132 | 144 | 156 | 168 | 180 | 168 |
| $\{\gamma_z\}_{95}^{\text{down}} (\text{m/s}^2)$ | 5.15 | 4.24 | 3.64 | 3.06 | 2.47 | 1.95 | 3.78 |
| $\{\gamma^{\text{app}}\}_{95}^{\text{down}} (\text{m/s}^2)$ | 5.15 | 4.54 | 3.93 | 3.33 | 2.72 | 2.11 | 4.10 |

behavior of this type of HSL in terms of acceleration is analyzed herein. In particular, the influence of temperature and thickness of the asphalt layer is highlighted.

Asphalt materials are thermo-sensitive and have a viscoelastic behavior, which is modeled here according to the Huet–Sayegh model presented in Section 3. The parameter values for the considered bituminous mix are displayed in Table IV. In the present example, the layer of asphalt material is part of a track bed composed of four layers (Table V) and is positioned under the ballast layer (which is the topmost layer of the structure). The considered loading and the rail/sleeper system are the same as previously. The speed is set to $V=95$ m/s in the ViscoRail computations.

Figure 10 presents the time evolutions of γ_z in the ballast layer as a function of the thickness of the asphalt layer, e , for a point located under a sleeper center. These curves are obtained for a uniform temperature $\theta=15^\circ\text{C}$. The thickness of the asphalt layer is varied from 0.05 to 0.20 m; higher values of the thickness leading to lower γ_z , as expected from the previous section. In particular, Figure 10 shows that for a thickness of 0.15 m the vertical acceleration in the ballast layer ($V=95$ m/s) is similar to that of the reference case corresponding to $V=75$ m/s.

It is worth noting that this viscoelastic computation can be approximated by a fully elastic one provided a right choice for the Young modulus (E_{eq}) of the asphalt material. In the present case, E_{eq} is found to be of this order of 12,000 MPa that corresponds to the norm of the complex modulus (parameters given in Table IV) computed for $\theta=15^\circ\text{C}$ and a frequency $f=15$ Hz. As a comparison, the equivalent elastic modulus used to model asphalt materials in the French pavement design method is obtained for $\theta=15^\circ\text{C}$ and $f=10$ Hz (corresponding to a smaller deflection basin but also to a lower speed of about 20 m/s).

Table IV. Values of the Huet–Sayegh parameters.

| E_∞ (MPa) | E_0 (MPa) | k | h | δ | τ_0 (s) | A_1 ($^\circ\text{C}^{-1}$) | A_2 ($^\circ\text{C}^{-1}$) |
|------------------|-------------|-------|-------|----------|--------------|---------------------------------|---------------------------------|
| 32665 | 11 | 0.193 | 0.592 | 2.244 | 18.973 | -0.397 | 0.00195 |

Table V. Materials properties of the viscoelastic track bed.

| | ρ (kg/m ³) | E (MPa) | ν | Thickness (m) |
|------------------|-----------------------------|--------------------|-------|---------------|
| Ballast | 1800 | 150 | 0.4 | 0.3 |
| Asphalt material | 2400 | N/A (viscoelastic) | 0.35 | Varied |
| Sub-layer | 1800 | 120 | 0.4 | 0.2 |
| Soil | 1800 | 100 | 0.4 | ∞ |

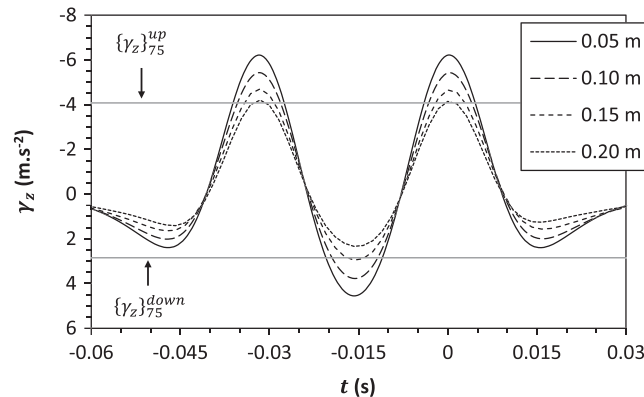


Figure 10. Time evolution of γ_z in the ballast layer for a point located right under a sleeper center: influence of the thickness of the sub-ballast asphalt layer ($V=95$ m/s, $\theta=15^\circ\text{C}$, $z=0.05$ m).

Because bituminous materials are thermo-sensitive, the influence of temperature on the vertical acceleration in the ballast layer is also studied and shown in Figure 11. The computations are performed for $V=95$ m/s, and the thickness of the asphalt layer is set to 0.15 m. The temperature is varied in the range from 0 to 45 °C. As expected, γ_z increases with temperature because the asphalt material softens as temperature increases. For instance, at $\theta=45$ °C γ_z is of the order of that obtained for $\theta=15$ °C and $e=0.05$ m.

These results show that the insertion of an asphalt layer in the track bed is probably a suitable solution to reduce geometrical disorders in the ballast, provided that this layer is adequately designed with respect to its temperature variation under the ballast. Consequently, design studies should take into account the expected *in situ* temperature histograms possibly coupled to those of traffic.

The design of the asphalt layer must also integrate the fatigue damage induced by tensile strain. Figure 12 shows for different temperatures the time evolution of the longitudinal (ϵ_{xx}) and transversal (ϵ_{yy}) strains computed at the bottom of the asphalt layer for $e=0.15$ m. Positive values correspond to tensile strains. In the present case, the maximum values are obtained in the transversal direction. These values can be used to estimate the life duration of the asphalt layer, in particular taking advantage of the knowledge gained from the road sector.

For example, considering the French pavement design method and climatic conditions leading to a design temperature equal to θ_{design} in the bituminous materials, the life duration of the asphalt layer

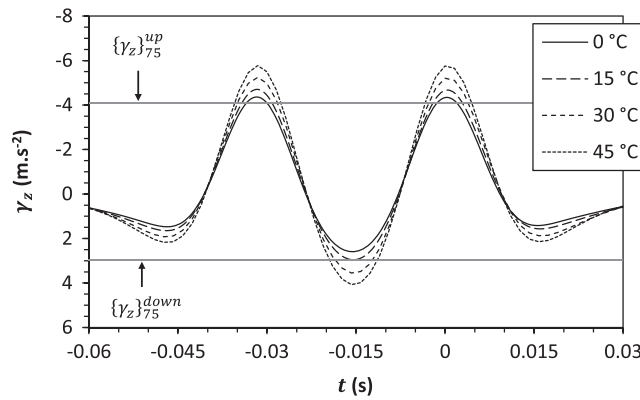


Figure 11. Time evolution of γ_z in the ballast layer for a point located right under a sleeper center: influence of the temperature in the asphalt layer ($V=95$ m/s, $e=0.15$ m, $z=0.05$ m).

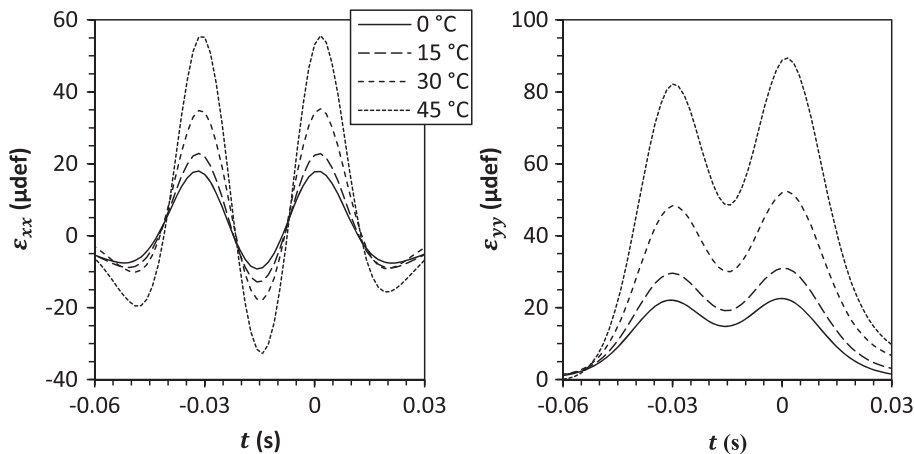


Figure 12. Time evolution of ϵ_{xx} and ϵ_{yy} at the bottom of the asphalt layer for a point located right under a sleeper center: influence of temperature ($V=95$ m/s, $e=0.15$ m, $z=0.45$ m).

may be deduced from Eq. (8) that relates the maximal admissible strain $\varepsilon_{t, adm}$ to the number NE of load passages:

$$\varepsilon_{t, adm} = \varepsilon_6(10^\circ\text{C}, 25 \text{ Hz}) \times \sqrt{\frac{|E^*|(10^\circ\text{C}, 10 \text{ Hz})}{|E^*|(\theta_{\text{design}}, 10 \text{ Hz})}} \times \left(\frac{NE}{10^6}\right)^b \times k_c \times k_s \times k_r \quad (8)$$

with

- $\varepsilon_6(10^\circ\text{C}, 25 \text{ Hz})$: strain level leading to a life duration of 10^6 cycles for trapezoidal samples tested according to the normalized fatigue test (NF EN 12697–24).
- b : slope of the fatigue law ($-1 < b < 0$)
- $|E^*|(10^\circ\text{C}, 10 \text{ Hz})$: norm of the complex modulus at 10°C and 10 Hz
- $|E^*|(\theta_{\text{design}}, 10 \text{ Hz})$: the same as above for θ_{design}
- k_c , k_s , and k_r : scaling factors depending upon the type of bituminous material, the stiffness of the sub-layer and the percentage of risk level accounted for the design project.

Considering for instance a material of type GB4 according to French standards leads to the following figures: $\varepsilon_6 = 100 \mu\text{def}$, $b = -0.2$, $k_c = 1.18$ after correction of the standard value 1.40 because of the absence of wandering in the case of railways, $k_s = 1$ for $E_{\text{sub-layer}} \geq 120 \text{ MPa}$ and k_r computed for a risk of 1%.

Then inverting Eq. (8) for $\varepsilon_{t, adm} = 34 \mu\text{def}$ deduced from the curve ε_{yy} at 15°C (Figure 12) and Miner's law to assimilate the two peaks of a bogie to a single load passage, we obtain $NE \approx 340 \times 10^6$ axle passages of 160 kN, or still 17×10^6 usual high-speed trains.

Note also that another design criterion to be considered is the vertical stress applied to the soil. In a different context, Teixeira [22], for example, recommends the use of an asphalt layer of thickness 0.12 to 0.14 m to obtain a compressive σ_{zz} in the soil equivalent to that of a classic all-granular track bed.

7. CONCLUSIONS

As suggested by field feedbacks and laboratory testing, the rapid geometrical deterioration of ballast layers of HSL seems to be in relation with the recent increase of train speed. This advocates the idea that the vertical acceleration into the ballast can explain in part this phenomenon by inducing a decrease of the granular assembly apparent weight. In consequence, a way to limit geometrical deterioration is to act directly on the HSL design to mitigate the ballast vertical acceleration generated by train passages.

In this context and on the basis of numerical simulations performed with ViscoRail, the influence of train speed and the role of inertia effects on the vertical accelerations computed in the ballast layer were analyzed. The rapid increase of the vertical accelerations with the train speed was especially evidenced (close to a function of the speed square). The effects of some structural parameters on acceleration were also quantified with intent to propose design solutions able to bring down accelerations computed at high speed to those of a reference case assumed non-problematic in terms of deterioration because of lower speed basically. It was shown that decreasing the stiffness of the mechanical connection between the rails and the ballast, increasing the moment of inertia of rails or the Young modulus of the sub-ballast layer, leads to a decrease of the vertical acceleration of ballast. Taking advantage of the capabilities of ViscoRail to account for viscoelastic materials, a particular solution that consists in inserting an asphalt sub-ballast layer was examined; this type of solution is already experimented in some sites worldwide including instrumented sections that should help better investigate the effect of stiffening the track bed.

REFERENCES

1. Shenton MJ. Deformation of railway ballast under repeated loading conditions. In *Railroad Track Mechanics and Technology*. Pergamon Press: Oxford, England, 1978; 405–425.
2. Hettler A. Bleibende setzungen des schotteroberbaues. *Eisenbahn-technische Rundschau* 33, H.11 1984.

3. Bodin, V. Comportement du ballast des voies ferrées soumises à un chargement vertical et latéral. PhD Thesis, Ecole Nationale des Ponts et Chaussées. 2001.
4. Guérin N. Approche expérimentale et numérique du comportement du ballast des voies ferrées. PhD Thesis, Ecole Nationale des Ponts et Chaussées. 1996.
5. Guérin N, Sab K, Moucheron P. Identification expérimentale d'une loi de tassement du ballast. *Canadian Geotechnical Journal* 1999; **36**(3):523–532.
6. Al Shaer, A. Analyse des déformations permanentes des voies ferrées ballastées – approche dynamique. PhD Thesis, Ecole Nationale des Ponts et Chaussées. 2005.
7. Al Shaer A, Duhamel D, Sab K, Foret G, Schmitt L. Experimental settlement and dynamic behavior of a portion of ballasted railway track under high speed trains. *Journal of Sound and Vibration* 2008; **316**(1–5):211–233. doi:10.1016/j.jsv.2008.02.055.
8. Oviedo X. Etude du comportement du ballast par un modèle micromécanique (application aux opérations de maintenance de la voie ferrée ballastée). PhD Thesis, Ecole Nationale des Ponts et Chaussées. 2001.
9. Foret G, Oviedo X, Sab K, Gautier PE. Vibration du ballast ferroviaire. *Revue Française de Génie Civil* 2003; **7**(6):777–795. doi:10.1080/12795119.2003.9692522.
10. Karrech A. Comportement des matériaux granulaires sous vibration – application au cas du ballast. PhD Thesis, Ecole Nationale des Ponts et Chaussées. 2007.
11. Quezada JC. Mécanismes de tassement du ballast et sa variabilité. PhD Thesis, Université Montpellier II. 2012.
12. Chupin, O. and Piau, J.M. Modeling of the dynamic response of ballast in high-speed train structures. In: *Proceedings of the 8th International Conference on Structural Dynamics. EURODYN* 2011. Leuven, Belgium, pp. 712–718. 2011.
13. Chupin O, Martin A, Piau JM, Hicher PY. Calculation of the dynamic response of a viscoelastic railway structure based on a quasi-stationary approach. *International Journal of Solids and Structures*. 2014. doi:10.1016/j.ijsolstr.2014.02.035.
14. Chabot A, Chupin O, Deloffre L, Duhamel D. ViscoRoute 2.0: a tool for the simulation of moving load effects on asphalt pavement. *Road Materials and Pavement Design* 2010; **11**(2):227–250.
15. Chupin O, Chabot A, Piau JM, Duhamel D. Influence of sliding interfaces on the response of a layered viscoelastic medium under a moving load. *International Journal of Solids and Structures*. 2010; **47**(25–26):3435–3446.
16. Duhamel, D., Chabot, A., Tamagny, P. and Harfouche, L. “ViscoRoute”: viscoelastic modeling for asphalt pavements. *Bulletin des Laboratoires des Ponts et Chaussées*, (258–259), pp.89–103. 2005.
17. Huet, C. Etude par une méthode d'impédance du comportement viscoélastique des matériaux hydrocarbonés. PhD thesis, Université de Paris. 1963
18. Sayegh, G. Contribution à l'étude des propriétés viscoélastiques des bitumes purs et des bétons bitumineux. PhD Thesis, Faculté des Sciences de Paris. 1965.
19. Martin A, Chupin O, Piau JM, Hicher PY. Deterioration of track geometry in ballasted high speed line: modeling approach and parametric study. In *Proceedings of the Ninth International Conference on the Bearing Capacity of Roads, Railways and Airfields*, Trondheim, Norway, 2013.
20. Robinet, A. L'expérience grave-bitume de la LGV Est Européenne. In: *Symposium international Géotechnique ferroviaire GEORAIL* 2011. Paris, France, pp. 477–484.
21. Rose, J.G., Teixeira, P.F. and Veit, P. International design practices, applications and performances of asphalt/bituminous railway trackbeds. In: *Symposium international Géotechnique ferroviaire. GEORAIL* 2011. Paris, France, pp. 99–119. 2011.
22. Teixeira PF *et al.* Improvements in high-speed ballasted track design: benefits of bituminous subballast layers. *Transportation Research Record: Journal of the Transportation Research Board* 19432006:43–49.